Journal of Alloys and Compounds 509 (2011) 3089–3095

Contents lists available at ScienceDirect

Journal of Alloys and Compounds

journal homepage: www.elsevier.com/locate/jallcom

Sinterability and microwave dielectric properties of nano structured $0.95MgTiO_3$–$0.05CaTiO_3$ synthesised by top down and bottom up approaches

M.A. Sanoj, C.P. Reshmi, K.P. Sreena, Manoj Raama Varma*

Materials and Minerals Division, National Institute for Interdisciplinary Science and Technology [NIIST], C.S.I.R., Thiruvananthapuram 695 019, India

ARTICLE INFO

Article history:
Received 30 June 2010
Received in revised form
30 November 2010
Accepted 1 December 2010
Available online 10 December 2010

Keywords:
MCT
Nanoceramics
Dielectric properties

ABSTRACT

$0.95MgTiO_3$–$0.05CaTiO_3$ (MCT) nano powders were synthesised using sol–gel method and high energy ball milling (HEBM). Synthesised powders were characterised using X-ray diffraction analysis to ensure phase purity and HRTEM to determine the fine microstructural features like particle size, interplanar spacing, etc. The powder pellets were heat treated to study the sinterability and microwave dielectric properties and these properties were then compared with the microwave dielectric properties of micron sized sample. Nano powder synthesised using HEBM shows better dielectric properties, sinterability and gets densified to 90% of theoretical density (TD) at 1200 °C/2 h. Dielectric resonators prepared using chemically synthesised nano powder showed poor sinterability and microwave dielectric properties, but, dielectric properties of HEBM samples were very near to that of solid state synthesised samples. Sintered HEBM powders retain the microwave dielectric properties almost to the same level as the solid state synthesised powder with considerable lowering of sintering temperature.

1. Introduction

Dielectric resonator materials are important in the miniaturization of microwave communication devices. To meet the requirements of miniaturization new developments in materials, integration and packaging are needed. In this context, low temperature co-fired ceramic (LTCC) technology has attracted much attention due to its capability of making three dimensional ceramic modules with low dielectric losses and embedded metal electrodes [1–4]. In LTCC Technology silver has widely been used as electrode material due its high electrical conductivity, comparatively moderate melting point (961 °C), easy processing and non reactivity with most of the dielectric resonator materials. But most of the dielectric resonator materials used in microwave frequency regime have high processing temperature (calcinations and sintering temperatures, sintering temperature > 1200 °C) [5]. Several techniques have been reported to minimize the processing temperature namely (a) addition of low melting glasses [6,7] and (b) chemical synthesis and use of powders with smaller particle size [8]. Low melting glass addition is found to be effective in lowering the sintering temperature by liquid phase sintering. But this process is known to deteriorate the dielectric properties [9]. However low cost and easy processing makes it an attractive option for making LTCC materials. The chemical synthesis decreases the sintering temperature considerably.

$MgTiO_3$ is a commonly used dielectric resonator material in the microwave frequency. Microwave dielectric properties of $CaTiO_3$ are also well known [5,9,10]. $MgTiO_3$ is known to have dielectric properties $\varepsilon_r \sim 17$, $Q \times f \sim 160{,}000$ GHz at 7 GHz and $\tau_f \sim -45$ ppm/°C and that of $CaTiO_3$ is $\varepsilon_r \sim 170$, $Q \times f \sim 3600$ at 7 GHz and $\tau_f \sim 800$ ppm/°C [5,10]. A composite $0.95MgTiO_3$–$0.05CaTiO_3$ (MCT) is reported to have $\varepsilon_r \sim 20$, $Q \times f \sim 56{,}000$ at 7 GHz and has near zero temperature coefficient of resonant frequency. Sintering temperature of this composite is reported as 1400–1500 °C [5,10]. Many researchers have made efforts to study the microwave dielectric properties of $0.95MgTiO_3$–$0.05CaTiO_3$ ceramics by various additives or by varying processing techniques. Recently Chen reported that addition of WO_3 has modified the microstructure and microwave dielectric properties of MCT [11]. He has also studied the effect of ZnO and V_2O_5 addition on the microwave dielectric properties of $0.85MgTiO_3$–$0.15Ca_{0.6}La_{0.8/3}TiO_3$ [12] and $0.8(Mg_{0.95}Zn_{0.05})TiO_3$–$0.2Ca_{0.61}Nd_{0.26}TiO_3$ ceramics [13] respectively and observed the possibilities of tuning microwave dielectric properties by controlling the additive amount. Extensive studies have been carried out by Chen on modified MCT ceramics with modifications done by substituting different elements in the Mg, Ca and Ti sites of MCT systematically [13–20]. In the place of Mg in $MgTiO_3$, elements like Zn [14,15], Co [16], La [17,18] and Nd [19] were substituted. In the place of Ti too, substitution of Mg and Ti in 1:1 ratio was done [18,19]. For $CaTiO_3$, substitution of Ca site was

* Corresponding author. Tel.: +91 471 2515377; fax: +91 471 2491712.
E-mail addresses: manoj@niist.res.in, manojraamavarma@yahoo.co.uk (M.R. Varma).

0925-8388/$ – see front matter © 2010 Elsevier B.V. All rights reserved.
doi:10.1016/j.jallcom.2010.12.006

done with Zn [16], Sr [14,18,19], Nd [20] and also with La–Na [15] and Nd–Na [17] in 1:1 ratios. All these substitutions gave sintering temperature in the range of 1150–1500 °C and microwave dielectric properties $\varepsilon_r \sim 19$–45 with maximum possible value of 132 [19], $Q \times f \sim 9500$–68,000 GHz and $\tau_f \sim 8.9$ to −14.9 ppm/°C [12,13]. Dielectric materials prepared by flexible chemical techniques could be sintered at lower temperatures and showed excellent dielectric properties of $Q \times f = 73{,}700$ at 6.5 GHz [21].

Even though a large number of papers are already published on the microwave dielectric properties of MCT ceramics, effect of different synthesis processes on the particle size and microwave dielectric properties of MCT was not reported before. In the present investigation particle size and sinterability of nano powders of MCT, prepared via two different well established routes such as chemical synthesis and high energy ball milling (HEBM) are compared with the MCT synthesised by conventional solid state method. Microwave dielectric properties of the sintered samples are also compared.

2. Experimental

2.1. Preparation of $0.95MgTiO_3$–$0.05CaTiO_3$ (MCT)

2.1.1. Solid state route

$MgTiO_3$ and $CaTiO_3$ were individually synthesised using the conventional solid state ceramic route using high purity Magnesium Carbonate [$(MgCO_3)_4Mg(OH)_2{\cdot}5H_2O$ Sigma–Aldrich, USA 99.9%], Calcium Carbonate ($CaCO_3$, Sigma–Aldrich, USA 99.9%) and Titanium Dioxide (TiO_2, Sigma–Aldrich, USA 99.9%). For the synthesis of $MgTiO_3$ and $CaTiO_3$ by solid state route carbonates of magnesium, calcium and oxide of titanium were accurately weighed and mixed with distilled water and subjected to ball milling with zirconia balls for 24 h. The slurry was dried and calcined at 1100 °C/4 h. Stoichiometric quantities of $MgTiO_3$ and $CaTiO_3$ were weighed accurately and mixed in a ball mill for getting $0.95MgTiO_3$–$0.05CaTiO_3$. The slurry was then dried with the addition of 3 wt% polyvinyl alcohol (as binder) and pressed in the form of circular discs of diameter 14 mm at height 7 mm. These discs were sintered at different temperatures to optimize the sintering temperature. Sintered pellets were used for dielectric characterization and structural analysis.

2.1.2. Sol–gel synthesis

For the synthesis of MCT by sol–gel method, $MgTiO_3$ and $CaTiO_3$ were prepared individually and mixed in the stoichiometric proportion. The starting materials used for the synthesis were $Ca(NO_3)_2{\cdot}4H_2O$ (Sigma–Aldrich, USA 99%), $Mg(NO_3)_2{\cdot}6H_2O$ (Sigma–Aldrich, USA 99.999%), $Ti[OCH(CH_3)_2]_4$ (Acros organics, 98+%), in the molar ratio Ca/Mg:Ti = 1:1. Solvent used for the synthesis was 2-methoxy ethanol (Sigma–Aldrich, USA). The stoichiometric quantities of the nitrates of Ca and Mg were dissolved in 30 mL and 50 mL of 2-methoxy ethanol respectively and stirred for 2 h at room temperature. Stoichiometric quantities of titanium isopropoxide were added to 10 mL of 2-methoxy ethanol taken in separate beakers and stirred for half an hour at room temperature. This solution was slowly added to the stirred solution of nitrates of Ca and Mg in 2-methoxy ethanol to get a transparent gel. The gel was dried at 70 °C for 24 h and calcined at 500 °C and 650 °C respectively [22–26] and then sintered at different temperatures.

2.1.3. High energy ball milling (HEBM)

The calcined powder of the MCT ceramics synthesised by solid state ceramics route was subjected to high energy ball milling for 20 h using a Fritsch Pulverisette P-5. The balls were of tungsten carbide (10 mm dia) and the ball to powder ratio was 10:1. The phase purity of the ball milled powder was ensured using X-ray diffraction patterns taken after every 5 h of ball milling using Cu Kα radiation (of wavelength, λ 1.54056 Å, Philips X'pert system) for a 2θ range 10–80°.

2.2. Characterization of powders and sintered samples

The crystallite size (d) of the nano MCT powder was determined from the XRD patterns using Debye Scherrer's formula $d = (0.9\lambda)/((\beta - \beta')\cos\theta)$, where λ is the wavelength of the X-ray, β and β' are the FWHM of the maximum intensity peak of the nano MCT powder and the reference sample respectively and θ is the glancing angle [27,28]. Solid state synthesised, sintered and well annealed sample was used as the reference. MCT nano particles were characterised using a high resolution transmission electron microscope (HRTEM) (FEI Technai G^2 30S-TWIN machine operated at 300 kV). The particle morphology, size distribution, SAD patterns and high resolution lattice images were recorded using HRTEM.

The dimensional changes of the disc shaped samples during sintering were studied using a horizontal loading dilatometer with alumina rods and bat (Model DIL 402PC, NETZSCH Instruments, Germany). Discs were sintered at different temperatures and the microstructure studies of the sintered samples were done using scanning electron microscope (JEOL, 5600LV, Tokyo, Japan). SEM images recorded were analysed using image analysis software (Leica Qwin). The low frequency dielectric measurements were carried out using LCR meter (Hioki 3532-50 LCR Hi-Tester). The dielectric properties of the materials were measured in the microwave frequency (2–6 GHz) range using a network analyzer HP 8510C (Hewlett-Packard, Palo Alto, CA). The dielectric constant ε_r was measured by the post resonator method of Hakki and Coleman modified by Courtney [29,30]. The error in ε_r measurement using this technique is usually less than ±1%. Usually, three samples are prepared in a batch corresponding to a particular composition and the measurements are made, at least twice per each specimen. The $TE_{01\delta}$ mode of resonance, where quality factor is intimately related to the dielectric loss ($tan\ \delta$), was used for the measurement of quality factor. The quality factor ($Q \times f$) was determined using a resonant copper cavity whose interiors were coated with silver and the ceramic dielectric was placed on a low loss quartz spacer, which reduces the effect of losses due to the surface resistivity of the cavity. For measuring quality factor, the resonant cavity method is ideal since the electric field is symmetrical with geometry of the cavity and the dielectric. The coefficient of thermal variation of resonant frequency (τ_f) was measured by noting down the temperature variation of the resonant frequency of $TE_{01\delta}$ mode in the reflection configuration over a range of temperature 20–80 °C, when the sample was kept in the end shorted position. The temperature coefficient of the resonant frequency was calculated using the formula $\tau_f = (f_2 - f_1)/(f_1(T_2 - T_1))$ where, f_1 and f_2 were the resonant frequencies at temperatures T_1 and T_2 and the average value was calculated and reported to be [9,31,32].

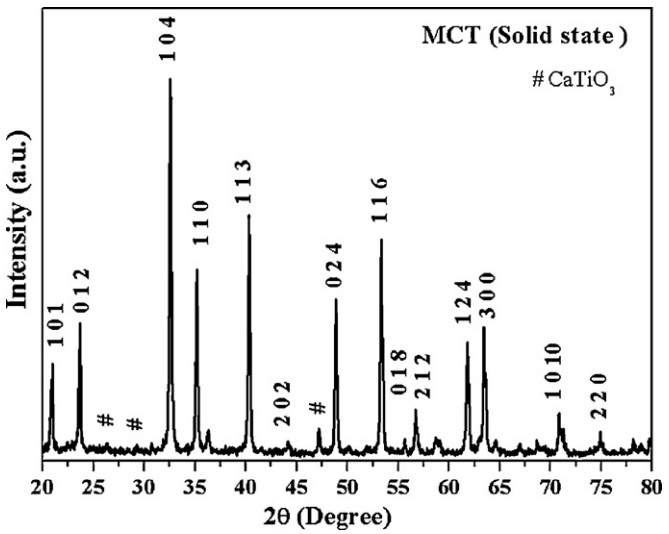

Fig. 1. X-ray diffraction (XRD) pattern of MCT ceramics synthesised using solid state method and sintered at 1350 °C/2 h.

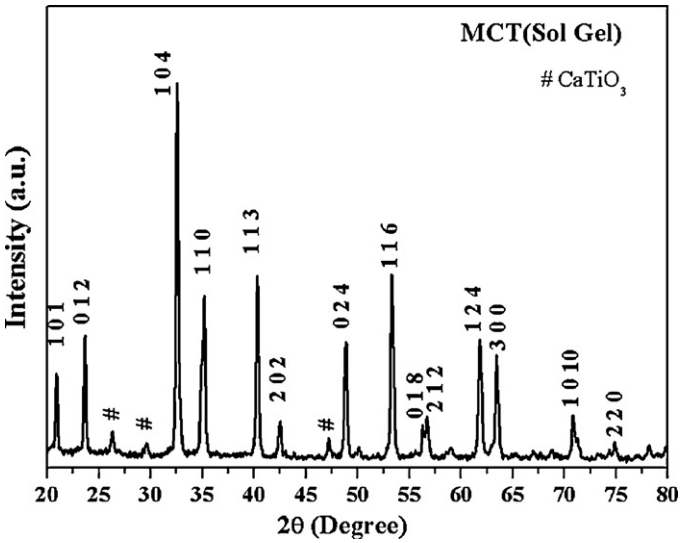

Fig. 2. X-ray diffraction (XRD) pattern of MCT ceramics synthesised using sol–gel method and sintered at 1300 °C/2 h.

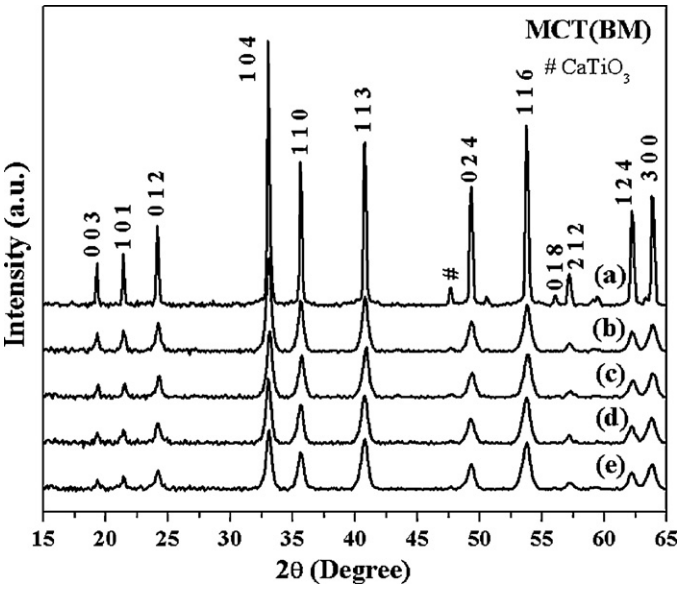

Fig. 3. X-ray diffraction (XRD) pattern of MCT ceramics synthesised by HEBM. (a) Before ball milling, (b) ball milled for 5 h, (c) 10 h, (d) 15 h and (e) 20 h.

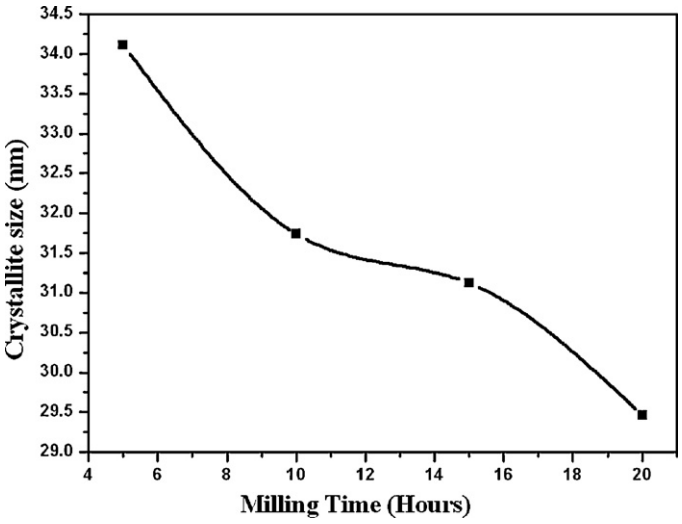

Fig. 4. The variation of crystallite size calculated from XRD patterns of HEBM sample with milling time.

3. Results and discussion

Figs. 1 and 2 represent the powder X-ray diffraction (XRD) patterns of MCT ceramics synthesised using solid state method, sintered at 1350 °C/2 h and sol–gel method, sintered at 1300 °C/2 h respectively. Fig. 3 is the XRD pattern of MCT solid state synthesised and high energy ball milled (a) before ball milling, (b) ball milled MCT ceramics at 5 h, (c) 10 h, (d) 15 h and (e) 20 h. The recorded XRD patterns are compared with the standard ICDD data files (File No. 79-0831 for $MgTiO_3$ and 43-0226 for $CaTiO_3$) and all the peaks were indexed accordingly. No secondary phases are present in the X-ray diffraction pattern and hence it is concluded that MCT forms as a mixture of both $MgTiO_3$ and $CaTiO_3$. XRD pattern of HEBM powders clearly indicates that no contamination of the charged powder with ball material (tungsten carbide) takes place during the HEBM process even for the longest duration of 20 h. As the milling time is increased the peaks get broadened showing a reduction in the diffraction domain size. The crystallite size of HEBM synthesised MCT powders calculated using Debye Scherrer formula for different milling durations show a decrease in crystallite size with milling duration as shown in Fig. 4. The crystallite size is reduced to ~30 nm on milling for 20 h.

High resolution transmission electron micrographs (HRTEM) and selected area electron diffraction (SAED) pattern of $MgTiO_3$, $CaTiO_3$ and MCT synthesised through sol–gel synthesis are shown in Figs. 5, 6 and 7 respectively. The particle size of sol–gel synthesised $MgTiO_3$ and $CaTiO_3$ powders are in the range 20–30 nm. The particle size of MCT prepared by mixing sol–gel synthesised $MgTiO_3$ and $CaTiO_3$ also lies in the same range. Inter planar spacing of the visible lattice planes are determined from the lattice images of MCT (Fig. 7), are 4.11 Å and 4.88 Å corresponding to the (1 0 1) and (0 0 3) planes respectively. Fig. 8 shows the particle size distribution and the high resolution image of the MCT particles synthesised using HEBM. The particle size obtained from the TEM image was less than about 20 nm. The TEM image analysis reveals that the particle size of MCT samples synthesised via two different methods are in the nanometre regime and the particle size obtained for MCT synthesised using HEBM method is the smallest (for 20 h of ball milling).

Fig. 9 depicts the effect of temperature on shrinkage ($\Delta L/L_0$) of MCT ceramics synthesised via three different methods studied using dilatometer. The shrinkage for the nano particle compacts

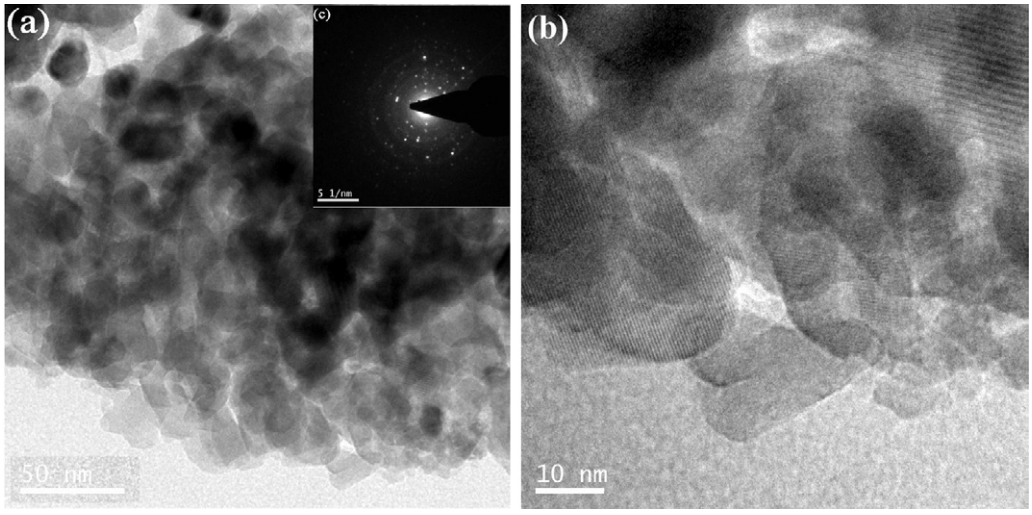

Fig. 5. Transmission electron micrographs of $MgTiO_3$ synthesised by sol–gel method (a) particle size distribution, (b) high resolution image and (c) SAED pattern.

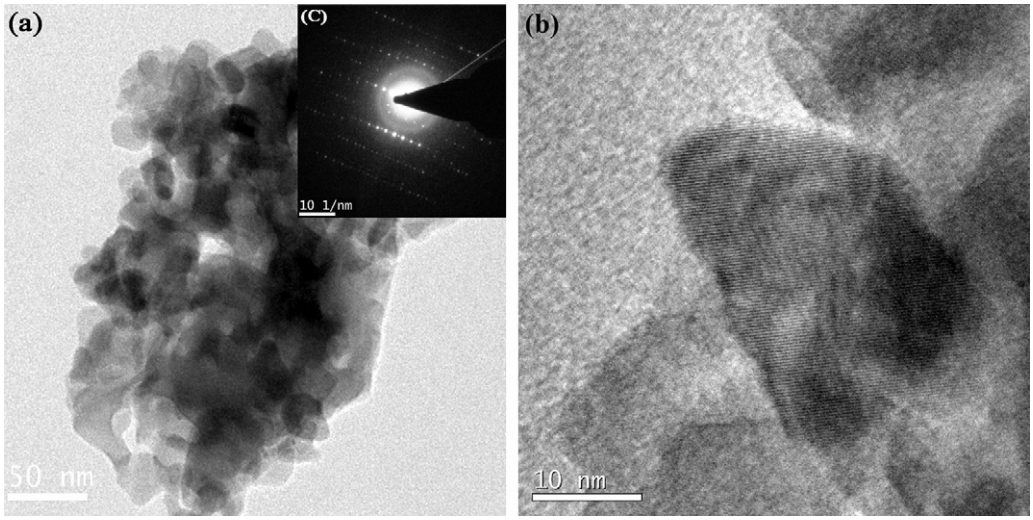

Fig. 6. Transmission electron micrographs of $CaTiO_3$ synthesised by sol–gel method (a) particle size distribution, (b) high resolution image and (c) SAED pattern.

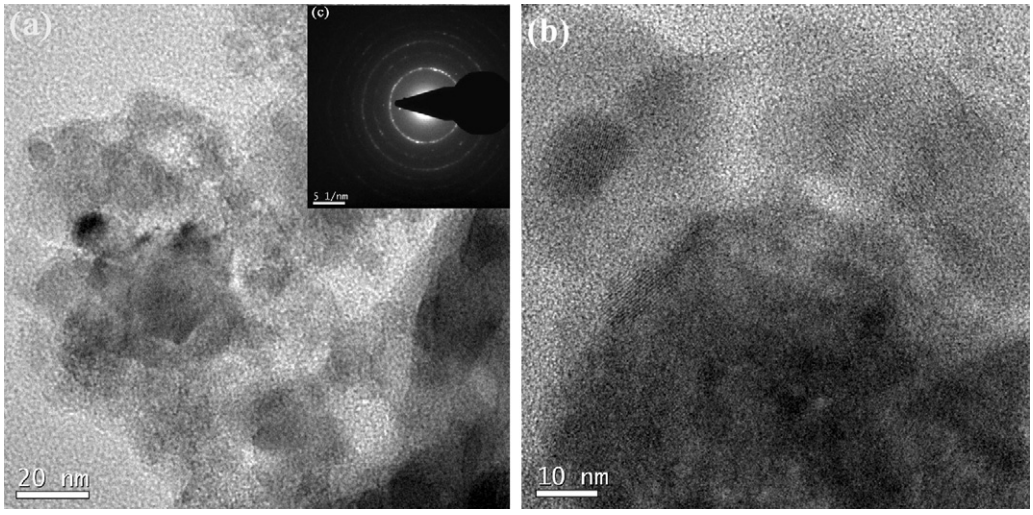

Fig. 7. Transmission electron micrographs of MCT synthesised by sol–gel method (a) particle size distribution, (b) high resolution image and (c) SAED pattern.

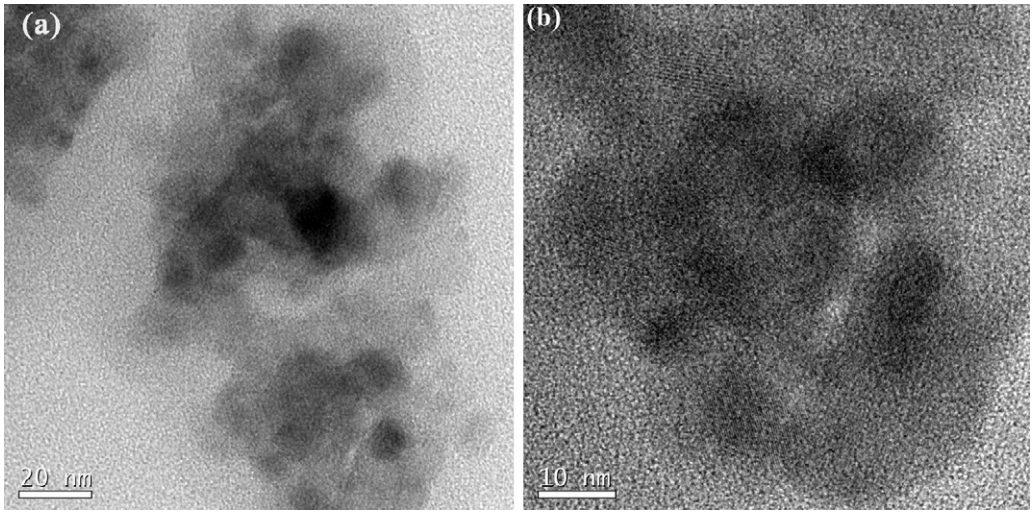

Fig. 8. Transmission electron micrographs of MCT synthesised by HEBM method (a) particle size distribution and (b) high resolution image.

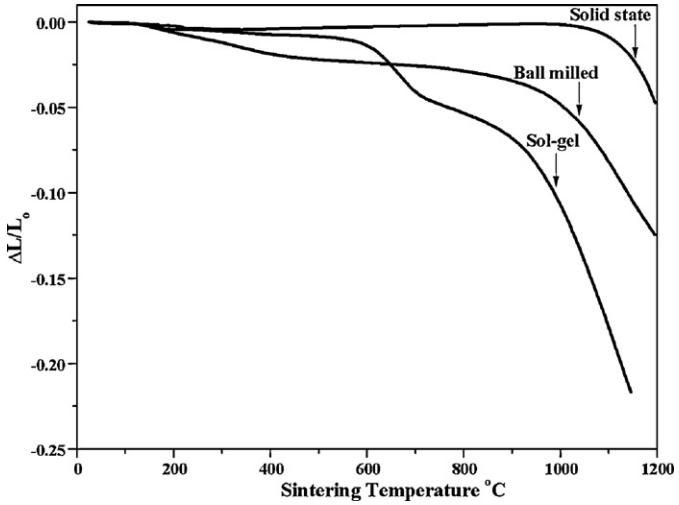

Fig. 9. Shrinkage of MCT ceramic pellets synthesised by different method with temperature.

begins at much lower temperatures and progresses more rapidly in comparison with the micron sized compacts. For HEBM synthesised MCT, shrinkage starts at very low temperature ~300 °C and gradually increases up to ~800 °C, beyond this temperature a rapid shrinkage is obtained and the sample densifies at ~1200 °C. Similar behaviour is obtained for the sol–gel synthesised MCT ceramics. MCT ceramics synthesised by solid state method shows shrinkage only from ~1050 °C onwards and shrinkage become more rapid beyond ~1100 °C. Hence it is clear that the nano sized particle compacts exhibits higher sinterability and the grain growth appears to be starting at lower temperatures than that of the micron sized powder.

For comparison of sinterability and grain growth, SEM micrographs of partially densified MCT (HEBM) and MCT (SG) sintered at 1100 °C/2 h were recorded and an image analysis was carried out. Average grain diameters of MCT samples sintered at different temperatures are given in Table 1 Solid state synthesised samples did not get sintered at1100 °C/2 h and the samples were behaving like green pellets after the heat treatment. Grain growth behaviour is found to be different for sol–gel synthesised and HEBM synthesised powder compacts. Greater grain growth was observed in the samples synthesised by HEBM than the samples synthesised using sol–gel synthesis and sintered at 1100 °C. Average grain size of about 1.5 μm was observed in HEBM MCT ceramics and that for the sol–gel samples were less than 1 μm when subjected to the same heat treatment. Also large number of inter granular shrinkage porosities were observed in the SEM microstructure of sintered nano powders. These observations support the shrinkage behaviour of MCT powder compacts shown in Fig. 9.

Fig. 10 shows the microstructures of MCT (a) synthesised by conventional solid state ceramic technique and sintered at 1350 °C/2 h (b) synthesised by sol–gel technique and sintered at 1350 °C/2 h and (c) synthesised by high energy ball milling (HEBM) and sintered at 1350 °C/2 h. Image analysis results of these figures are also given in

Table 1
Variation of grain diameter of MCT ceramics with the sintering temperature from SEM images.

Sample ID	Average grain diameter (μm)	
	1100 °C	1350 °C
MCT (solid state)	Not sintered	5–6
MCT (high energy ball milled)	1.2–1.5	11–12
MCT (sol gel)	0.7–1.0	7–8

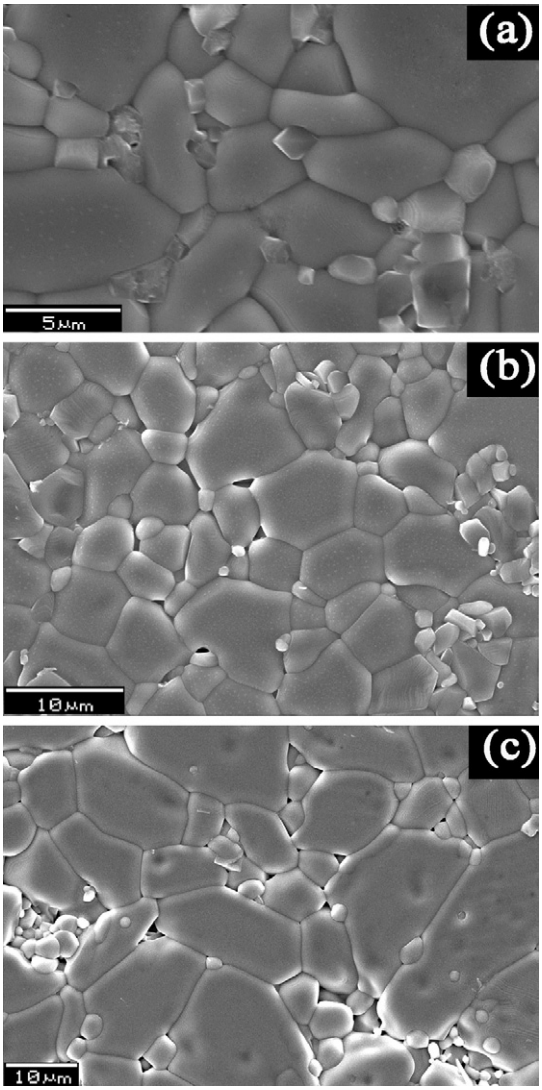

Fig. 10. Scanning electron micrographs of MCT synthesised by (a) conventional solid state method sintered at 1350 °C/2 h (b) sol–gel technique sintered at 1350 °C/2 h and (c) synthesised using HEBM and sintered at 1350 °C/2 h.

Table 1. From the SEM micrographs it is clear that all the samples are well densified. MCT ceramics synthesised by solid state synthesis technique had minimum porosity with an average grain diameter ~5–6 μm (Table 1). The average grain diameter of sol–gel synthesised sample sintered at 1350 °C was about 7–8 μm and that for HEBM sample was about 11–12 μm. Comparing these values it can be noticed that nano particles sintered samples have larger grain diameters. The main driving force for sintering in powder compacts is the tendency to reduce the surface free energy by reducing surface area. In the case of nano particle compacts, the total surface area per unit volume is much larger when compared to that of the micron sized powder compacts. Hence the shrinkage and grain growth rates are greater in nano powder compacts [33].

Fig. 11 shows the variation of the relative density with sintering temperature of MCT powder compacts synthesised by conventional solid state ceramic route, sol–gel synthesis and the HEBM techniques. Fastest densification kinetics can be observed for HEBM powders. HEBM sample is densified to 90% of theoretical density at 1200 °C. The lower particle size of ball milled samples helps them to have greater grain growth kinetics by reducing the total surface area. HEBM process is also known to introduce large amounts of dislocations and surface defects on the surface of nano powder

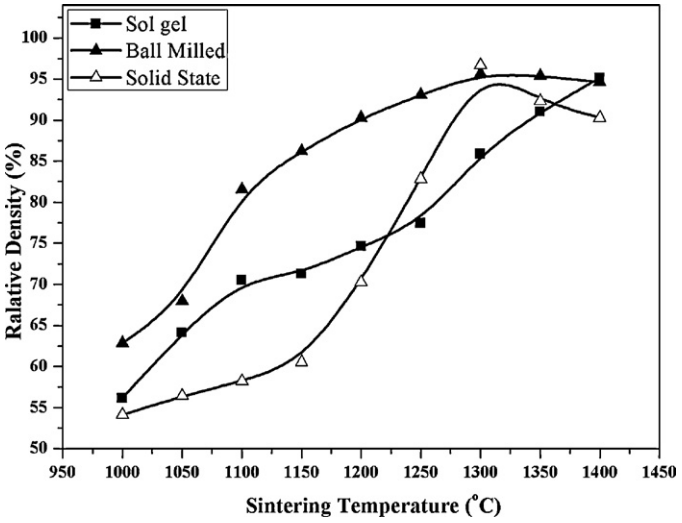

Fig. 11. Variation of relative density with sintering temperature.

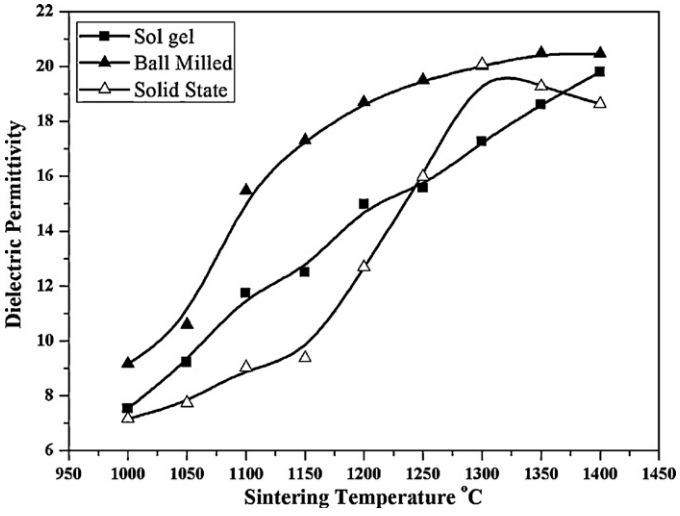

Fig. 13. Variation of dielectric permittivity with sintering temperature.

particles, which increase the sinterability of the powder compacts. This effect can be observed in the shrinkage behaviour in Fig. 9 and the microstructural analysis details given in Table 1. It can be seen from Fig. 11 that the densification of the solid state synthesised samples are slower than the HEBM synthesised sample at any given temperature. The densification with respect to the sintering temperature shows a sigmoidal dependence on temperature. This behaviour can be observed in the results of densification of MCT synthesised via conventional solid state synthesis technique and HEBM synthesis. Densification up to 96% of the theoretical density is observed for solid state synthesised samples. For HEBM maximum density achieved is around 95% of theoretical density. The difference between theoretical density and actual density measured using Archimedes principle gives the amount of internal porosity. In the case of solid state synthesised samples porosity present is about 4% and for HEBM samples it is 5%.

In the case of sol–gel samples, densification is very slow and reaches 90%TD only around 1350 °C/2 h. Generally chemically synthesised nano powders show a lower densification [8,9]. This is mainly due to the accommodation of shrinkage porosity in the intergranular regions. The porosity trapped in the intergranular regions prevents sol–gel powder compacts from acquiring high densities even at highest temperatures like 1400 °C/2 h and only 93% of theoretical density can be obtained (with 7% porosity). Fig. 12 shows the microstructure of the cross section of MCT ceramics

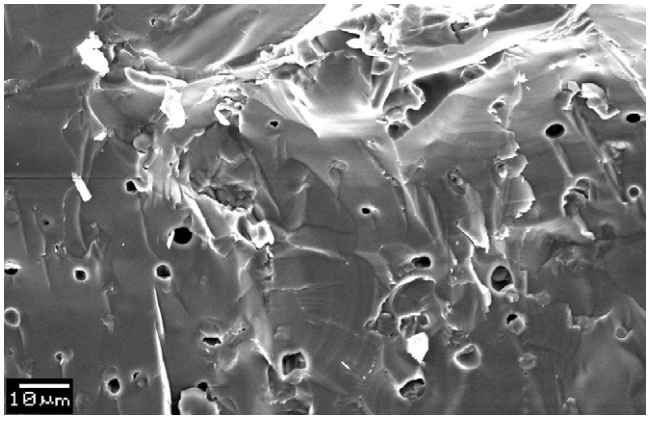

Fig. 12. SEM micrograph of fractured surface showing intergranular porosity of MCT (SG) ceramics sintered at 1250 °C/2 h.

Table 2
Microwave dielectric properties of MCT ceramics prepared through different techniques.

Sample ID	Sintering temperature (°C)	ε_r	$Q \times f$ (GHz)	τ_f (ppm/°C)
MCT(SS)	1350	17.2	60,800	−0.5
MCT (BM)	1200	17.2	24,100	−8.5
MCT (SG)	1350	16.4	16,750	−17.5

synthesised via sol–gel and sintered at 1250 °C/2 h. In the figure shrinkage porosity is clearly visible which strongly supports the lower density of the sintered samples. At higher sintering temperature some of these pores may get closed due to the mass transfer by diffusion, giving the final sintered microstructures as shown in Fig. 10.

Dependence of the dielectric permittivity, measured using LCR meter at low frequency (1 MHz), on sintering temperature of MCT synthesised by solid state, sol–gel and HEBM techniques are shown in Fig. 13. Dielectric permittivity mainly depends on polarization in the material and its variation shows similar trends as density variation showing highest values for HEBM samples. Dielectric permittivity of the solid state synthesised samples is almost same as that of HEBM samples. Inter granular porosity (around 7%) introduced in the sintering process of sol–gel synthesised samples reduces the dielectric permittivity as shown in Fig. 13.

Table 2 illustrates the microwave dielectric properties, quality factor ($Q \times f$) and temperature coefficient of resonant frequency (τ_f) of MCT synthesised by three different methods. Only HEBM synthesised MCT shows good resonance at lower sintering temperatures. Microwave dielectric properties of HEBM samples sintered at 1200 °C/2 h was found to be $\varepsilon_r = 17.2$, $Q \times f = 24{,}100$ GHz and $\tau_f = -8.5$ ppm/°C. With the increase in the sintering temperature the quality factor also increases and reaches a maximum value ($Q \times f = 52{,}000$ GHz) at a sintering temperature of 1350 °C/2 h. The samples synthesised via solid state and sol–gel method, sintered at lower temperatures do not show resonance (below 1300 °C). The samples synthesised by solid state method have microwave dielectric properties $\varepsilon_r = 17.2$, $Q \times f = 60{,}800$ GHz and $\tau_f = -0.5$ ppm/°C when sintered at 1350 °C/2 h. Chemically synthesised MCT ceramics shows dielectric properties $\varepsilon_r = 16.4$, $Q \times f = 16{,}750$ GHz and $\tau_f = -17.5$ ppm/°C when sintered at 1350 °C/2 h. Quality factor of a material increases with increase in grain size and decreases with increase in porosity and other defects present in the material as the grain boundaries and defects act as scattering centres for the microwave radiation. Porosity defect level (~4%) in the solid state

synthesised sample is found to be much lower and hence gave highest quality factor. Even though the densification is good, quality factor of the HEBM samples are marginally lower due to the presence of more intergranular porosities (5%). However the porosities in sol–gel powder sintered samples is more (7%) in the form of closed intergranular pores which is the main reason for the lowest quality factors.

4. Conclusions

MCT ceramics having compositions $0.95MgTiO_3$–$0.05CaTiO_3$ was prepared by conventional solid state ceramic route and the nano powders by sol–gel synthesis and high energy ball mill (HEBM) method. The crystallite size of the nano powders was determined using X-ray diffraction and the particle sizes of the nano powders were determined using high resolution transmission electron microscopy (HRTEM). The particle size obtained for HEBM sample is about 20 nm and that for sol–gel sample is up to 50 nm. The sinterability of micron sized and nano sized powder compacts were compared and correlated with its dielectric properties. The sample synthesised using HEBM shows excellent sinterability and comparatively good microwave dielectric properties at lower sintering temperature. The MCT ceramics obtained after HEBM show more than 90% densification at a sintering temperature of 1200 °C/2 h with dielectric properties $\varepsilon_r = 17.2$, $Q \times f = 24{,}100$ GHz and $\tau_f = -8.5$ ppm/°C, where as the sintering temperature of solid state and sol–gel is above 1300 °C. At this sintering temperature the microwave dielectric properties for solid state sample is $\varepsilon_r = 17.2$, $Q \times f = 60{,}800$ GHz and $\tau_f = -17.5$ ppm/°C. It can be concluded that HEBM is a good synthesis technique for the preparation of nano dielectric ceramics. Samples synthesised using this method is densified at lower temperatures and show microwave resonance at lower sintering temperature in comparison with the sol–gel and solid state synthesised samples. However temperature coefficient of resonant frequency of the nano powder sintered samples was much more than solid state synthesised samples (which is near to zero).

Acknowledgements

Authors would like to thank Department of Science and Technology, Government of India for supporting this project on LTCC and providing HRTEM facility in NIIST, CSIR, Thiruvananthapuram.

References

[1] S. George, M.T. Sebastian, J. Alloys Compd. 473 (2009) 336–340.
[2] H. Zhou, X. Chen, L. Fang, D. Chu, J. Mater. Res. 25 (2010) 1235–1238.
[3] X. Jiao, C. Zhong, S. Zhang, X. Liu, B. Li, J. Mater. Sci. 45 (2010) 3331–3335.
[4] C.L. Huang, J.L. Hou, C.L. Pan, C.Y. Huang, C.W. Peng, C.H. Wei, Y.H. Huang, J. Alloys Compd. 450 (2008) 359–363.
[5] M.T. Sebastian, Dielectric Materials for Wireless Communication, Elsevier, 2008.
[6] R. Wang, J. Zhou, B. Li, L. Li, J. Alloys Compd. 490 (2010) 204–207.
[7] C. Bienert, A. Roosen, J. Eur. Ceram. Soc. 92 (2009) 2648–2653.
[8] M.A. Sanoj, C.P. Reshmi, M.R. Varma, J. Am. Ceram. Soc. 92 (2009) 2648–2653.
[9] M.A. Sanoj, M.R. Varma, J. Alloys Compd. 477 (2008) 565–569.
[10] X. Zhou, Y. Yuan, L. Xiang, Y. Huang, J. Mater. Sci. 478 (2009) 657–660.
[11] Y.B. Chen, J. Alloys Compd. 478 (2009) 657–660.
[12] Y.B. Chen, J. Alloys Compd. 477 (2009) 883–887.
[13] C.L. Huang, Y.B. Chen, C.F. Tasi, J. Alloys Compd. 454 (2008) 454–459.
[14] C.L. Huang, S.H. Lin, S.S. Liu, Y.B. Chen, S.Y. Wang, J. Alloys Compd. 503 (2010) 392–396.
[15] C.L. Huang, S.H. Lin, S.S. Liu, Y.B. Chen, J. Alloys Compd. 489 (2010) 541–544.
[16] C.L. Huang, Y.B. Chen, S.H. Lin, J. Alloys Compd. 477 (2009) 712–715.
[17] Y.B. Chen, J. Alloys Compd. 500 (2010) 190–194.
[18] Y.B. Chen, J. Alloys Compd. (2010), doi:10.1016/j.jallcom.2010.11.024.
[19] Y.B. Chen, J. Alloys Compd. (2010), doi:10.1016/j.jallcom.2010.11.006.
[20] C.L Huang, C.F. Tasi, Y.B. Chen, Y.C. Cheng, J. Alloys Compd. 453 (2008) 337–340.
[21] M.K. Suresh, J.K. Thomas, H. Sreemoolanadhan, C.N. George, A. John, S. Solomon, P.R.S. Wariar, J. Koshy, Mater. Res. Bull. 45 (2010) 761–765.
[22] O. Renoult, J. Boilot, F. Chaput, R. Papiernik, L.G. Hubert-Pfalzgraf, M. Lejeune, J. Am. Ceram. Soc. 75 (1992) 3337–3340.
[23] S. Holliday, A. Stanishevsky, Surf. Coat. Technol. 188-189 (2004) 741–744.
[24] M. Yu, J. Lin, Z. Wang, J. Fu, S. Wang, H.J. Zhang, Y.C. Han, Chem. Mater. 14 (2002) 2224–2231.
[25] H. Beltran, E. Cordoncillo, P. Escribano, J.B. Carda, A. Coats, A.R. West, Chem. Mater. 12 (2000) 400–405.
[26] A.K. Cheetham, C.F. Mellot, Chem. Mater. 9 (1997) 2269–2279.
[27] S.C. Tjong, H. Chen, Mater. Sci. Eng. R. R 45 (2004) 1–88.
[28] A.P. Hynes, R.H. Doremus, R.W. Siege, J. Am. Ceram. Soc. 85 (2002) 1979–1987.
[29] B.W. Hakki, P.D. Coleman, IRE Trans. Microwave Theory Tech. MTT – 8 (1960) 402.
[30] W.E. Courtney, IEEE Trans. Microw. Theory Tech. MTT – 18 (1970) 476.
[31] H. Jantunen, R. Rautioho, A. Uusimaki, S. Leppavuori, J. Eur. Ceram. Soc. 20 (2000) 2331–2336.
[32] C.L. Huang, C.H. Shen, C.L. Pan, Mater Sci. Eng. B 145 (2007) 91–96.
[33] M.N. Rahaman, Ceramic Processing and Sintering, 2nd ed., CRC Publications, 2003.